International Journal of Current Trends in Engineering & Technology
ISSN: 2395-3152
Volume: 12, Issue: 01 (January-February, 2026)

# Utilization of $CO_2$ from a Carbon Capture Plant for Curing Alkali-Activated Low-Reactivity Fly Ash

Shubham Raghuvanshi [1], Arun Kumar Patel [2], Vishnu Prasad Dangi [3],
[1,2,3] Department of Civil Engineering, RKDF University, Bhopal, India
[1]shubhamrraghuvanshi@gmail.com, [2]arunpatel123@gmail.com, [3]vishnudangi1@gmail.com

## Abstract

Nowadays, the carbon dioxide ($CO_2$) capture and utilization for curing alkali-activated materials offer a promising pathway for both $CO_2$ sequestration and the production of low-carbon construction materials. However, low-reactive fly ash (FA), which is an easily accessible and widely available industrial byproduct. It poses basic challenges due to its poor reactivity under conventional curing conditions. In this research, the utilization of $CO_2$ generated from a pilot-scale carbon capture plant at RKDF University, Bhopal, is investigated to cure alkali-activated low-reactive FA pastes. The curing process is carried out at 40 °C and 0.5 bar gauge pressure for durations of 6, 12, and 24 h. Mass monitoring, compressive strength testing, X-ray diffraction (XRD), and efflorescence assessment are employed to evaluate the performance. The experimental results show that after 24 h of $CO_2$ curing, the pastes achieved a $CO_2$ uptake of 12.4 % by mass of FA. After 28 days, a compressive strength of 42.6 MPa is found, which is approximately 50% higher than that of ambient-cured controls. Efflorescence is nearly eliminated due to the conversion of free alkalis into insoluble carbonates. XRD analysis confirmed the formation of calcite ($CaCO_3$) as the primary carbonation product, while quartz and mullite remained inert. This research experimentally shows that $CO_2$ from a carbon capture plant can effectively upgrade low-reactive FA into a high-strength, durable material. It offers benefits of waste valorization, $CO_2$ storage, and utilization.

**Keywords:** Carbon Capture and Utilization (CCU), $CO_2$ Curing, Low-Reactivity Fly Ash, Alkali-Activated Materials, Geopolymer, Carbonation

## 1 Introduction

The cement and construction industries are responsible for approximately 8% of the global anthropogenic $CO_2$ emissions. It is primarily due to the calcination of limestone and the combustion of fossil fuels (Rootzén and Johnsson, 2017) [1]. The biggest challenge in the cement industries is to mitigate $CO_2$ emissions while still keeping up with and fulfilling the rising global demand. As developing economies expand their infrastructure, there is an urgent requirement to develop and implement modern technologies worldwide to mitigate emissions in this sector (Mehdizadeh and Hajmohammadian Baghban, 2025; Crispin, 2026) [2, 3].

The carbon capture and utilization (CCU) technologies have now emerged as a crucial strategy to mitigate $CO_2$ emission by carbon capture from point sources such as power plants and cement kilns. These plants capture $CO_2$ and convert it into value-added useful products (Harle *et al.*, 2026) [4]. There are various utilization pathways, the use of captured $CO_2$ for curing cementitious and alkali-activated materials has gained significant attention in the research. It definitely sequesters $CO_2$ permanently, as well as improves the physical and durability properties of the material (Llorente-García *et al.*, 2025; Chew *et al.*, 2025; Mora *et al.*, 2024) [5–7].

Alkali-activated materials (AAMs), commonly known as geopolymers, are basically low-carbon alternatives to the ordinary Portland cement (OPC) (Sun and Fan, 2024) [8]. They are typically produced by the reaction of the aluminosilicate precursors such as FA, slag, and metakaolin with an alkaline activator solution (Sirotti *et al.*, 2026; Khan *et al.*, 2025; Lukovic *et al.*, 2026) [9–11]. However, the widespread adoption of AAMs is hindered by the variable reactivity of industrial byproducts, particularly "low-reactivity FA," which is under Class F according to ASTM C618 [12]. Unlike high-calcium FA, low-reactive FA contains limited amorphous calcium phases, which results in slow setting, poor early-age strength, and susceptibility to efflorescence.

Fig. 1 illustrates the schematic representation of the integrated carbon capture and utilization (CCU) process to produce the alkali-activated low-reactivity FA products. The flue gas $CO_2$ is captured, purified, and then used for curing the FA paste, which finally yields a high-strength construction material. Fig. 2 represents the conceptual illustration of the microstructural changes induced by $CO_2$ curing. The uncured alkali-activated low-reactivity FA paste generally contains interconnected pores and free alkali ions (left). After the $CO_2$ curing process, the calcite precipitates fill the pores and consume alkalis, which finally leads to a highly dense, strong, and efflorescence-resistant material (right).

Recent research (Guo *et al.*, 2026; Wang *et al.*, 2026)

International Journal of Current Trends in Engineering & Technology
ISSN: 2395-3152
Volume: 12, Issue: 01 (January-February, 2026)

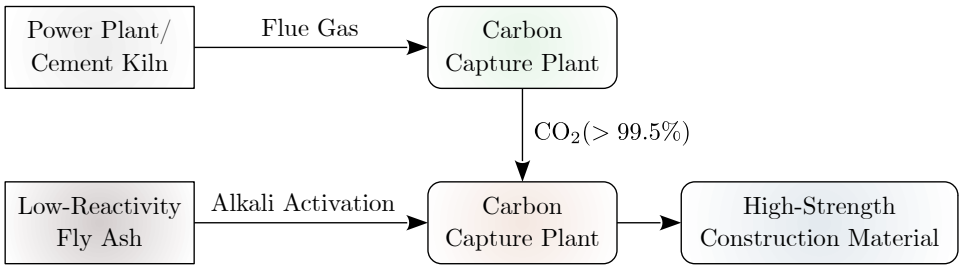


Fig. 1: Schematic Representation of CCU

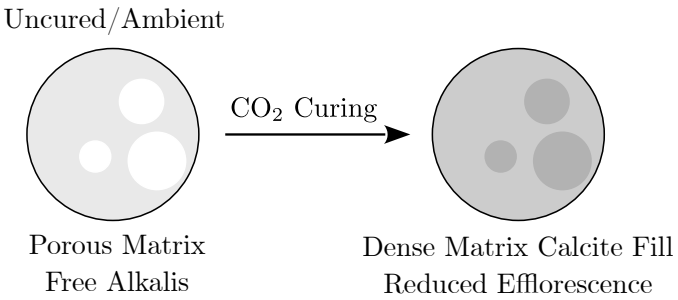


Fig. 2: Microstructural changes Induced by $CO_2$ Curing

[13, 14] has shown that $CO_2$ curing, which is also known as carbonation curing, can accelerate the reaction kinetics and enhance the performance of low-reactivity precursors. When $CO_2$ is introduced into an alkali-activated paste, it dissolves in the pore solution to form carbonate ions. After that, it reacts with calcium and sodium ions to precipitate calcite ($CaCO_3$) and sodium carbonate. This process enhances the density of the microstructure, increases strength, and consumes free alkalis; ultimately, it reduces the efflorescence. Nevertheless, most research has used pure $CO_2$ from gas cylinders, which is energy-intensive and does not reflect real-world CCU scenarios where $CO_2$ is supplied directly from a capture plant.

This research utilizes $CO_2$ generated from a pilot-scale carbon capture plant at RKDF University, Bhopal, for curing the alkali-activated pastes made from low-reactivity FA. The objectives of this research are as follows:

1. To quantify the $CO_2$ uptake and mass change as a function of curing time,
2. To evaluate the compressive strength development at 3, 7, 14, and 28 days,
3. To characterize the phase evolution using the XRD analysis,
4. To assess efflorescence resistance, and
5. To demonstrate the feasibility of direct CCU integration with the production of construction material.

The remainder of this paper is organized as follows: Section 2 represents comprehensive surveys on CCU, $CO_2$ curing, low reactivity FA, AAM, geopolymers, and their integrated researches. Section 3 describes the materials, sample preparation, and experimental methods. Section 4 presents the results and discussion of mass change, $CO_2$ uptake, compressive strength, XRD, efflorescence. Section 5 concludes the research and suggests directions for future work.

## 2 Related Work

In recent years, the curing of fresh concrete using $CO_2$ has been adopted as a carbon capture and storage (CCS) approach in response to the requirement to the mitigation of $CO_2$ emissions (Haselbach and Thomle, 2014; Lippiatt and Ling, 2020) [15, 16]. This section represents a comprehensive analysis on major application of carbon capture and its utilization in curing.

### 2.1 Carbon Capture and Utilization (CCU)

Carbon capture and utilization has been widely studied as a modern technology to mitigate the industrial $CO_2$ emissions while creating value-added products. The integration of CCU with construction materials has gained particular attention in the research (Mohammadi and Mousazadeh, 2022; Zhang *et al.*, 2022; Elaouzy and Zaabout, 2025) [17–19] due to the large potential for permanent $CO_2$ storage. Monoethanolamine (MEA)-based absorption is considered the most mature capture technology, though alternative solvents have been developed by Liang *et al.* (2015) [20] to minimize the energy losses.

Usta *et al.* (2022) [21] explored the production of sustainable building materials by carbonating the FA compacts. It basically served as sustainable building materials and achieved moderate strength (10-36 MPa) and significant $CO_2$ uptake (up to 15%). They found that the higher temperature, pressure, and $CO_2$ levels improved uptake, while compaction pressure enhanced strength and mixed ashes increased uptake but reduced strength.

Harirchi and Yang (2022) [22] examined the impact of $CO_2$ curing on low-reactive FA alkali-activated (geopolymer) pastes. $CO_2$ curing of FA geopolymers increases carbon uptake, with more $CO_2$ retained in the matrix over time. However, it hinders the geopolymerization, which causes the efflorescence and reduced strength, though longer curing maximizes the strength and improves the microstructure density.

Cuéllar-Franca and Azapagic (2015) [23] applied many life cycle assessment studies to compare the environmental impacts of CCS and CCU. They found that CCS significantly reduced the global warming potential (GWP) by 63-82%. However, it can increase other environmental impacts, such as acidification and human toxicity. CCU represented the application-specific mixed results, mineral carbonation and dimethyl carbonate production reduced GWP, while microalgae biodiesel increased it. CCS achieved greater GWP mitigation than most CCU options; however, CCU generally has a lower impact on other environmental categories.

Bui *et al.* (2018) [24] reviewed the current state of CCS, which covers capture, transport, utilisation, and storage across multiple scales. Although CCS is technically mature and vital for climate goals with net $CO_2$ removal. However, it has not been deployed up to the required scale due to its commercial and political barriers. They also examined the negative emissions technologies such as bioenergy with CCS and direct air capture, and highlighted the key research challenges and the obstacles to large-scale implementation.

## 2.2 Alkali-Activated Materials and Geopolymers

Alkali-activated materials (AAMs) are recognized as low-carbon alternatives to OPC in the research (Provis, 2018; Shi *et al.*, 2011) [25, 26]. The reaction mechanisms of FA-based geopolymers have been extensively characterized (Davidovits, 2020; Brooks *et al.*, 2010; Van Deventer *et al.*, 2012) [27–29]. However, the performance of AAMs strongly depends on the precursor reactivity [30, 31]. Low-calcium (Class F) FA, in particular, exhibits slow setting and low early strength in the research (Chindaprasirt *et al.*, 2009; Chi and Huang, 2013) [32, 33].

Xue and Hou (2024) [34] investigated the sustainable porous building materials made by alkali-activating FA with waste clay brick powder, which are capable of producing sustainable building materials. Approximately, 10% brick content represents the highest strength, while higher amounts reduce the strength but increase porosity, which makes it perfectly useful for insulation.

Zhu *et al.* (2025) [35] evaluated the hybrid alkali-activated cement (HAAC) in the form of a low-carbon alternative to OPC under accelerated curing. HAAC, which mainly contains the slag with some OPC, represents faster setting and higher strength, particularly at elevated curing temperatures. While higher curing temperatures increase energy use, the resulting strength gains reduce overall economic and environmental impacts that make moderate heat curing an efficient strategy for precast concrete production.

Dener *et al.* (2024) [36] found that the hybrid alkali-activated binders minimize $CO_2$ from OPC. They found optimal performance at 15% OPC in a moderate $Na_2SiO_3$/NaOH ratio, and 50℃ curing. They noted that the higher temperatures and excess OPC generally reduce the strength and hydration.

Schneider *et al.* (2025) [37] found that the submerged curing produced the best materials, which achieved $CO_2$ adsorption up to 2.24 mmol/g with high surface area and porosity. These geopolymers effectively capture $CO_2$ and can support reuse processes such as catalytic or electrochemical conversion. They concluded that the waste-based geopolymers are promising, cost-effective, and reusable materials for efficient $CO_2$ separation.

Bakri and Mahmoud (2026) [38] presented that geopolymer/alkali-activated binders perform much better. They maintained ultralow permeability and ∼90% strength under $CO_2$ exposure due to their stable gel structure and lack of portlandite. Unlike OPC, they resisted severe carbonation and pore damage. They found that the geopolymers are a more durable and sustainable alternative for $CO_2$ sequestration wells. However, the challenges remain in the mix design, consistency, and field validation.

## 2.3 $CO_2$ Curing of Cementitious and Alkali-Activated Systems

$CO_2$ curing (carbonation curing) has been characterized to enhance the physical properties and durability of concrete and AAMs in the research (Monkman and MacDonald, 2016; Ashok *et al.*, 2025; Oke and Abuel-Naga, 2025; Rostami *et al.*, 2012; Lei *et al.*, 2025) [39–43]. In the systems of OPC, the carbonation process leads to the formation of calcium carbonate and a densified the microstructure (Ren *et al.*, 2024; Fernández Bertos *et al.*, 2004) [44, 45]. For alkali-activated FA, $CO_2$ curing can promote the precipitation of calcite and consume free alkalis, thereby, it reduces efflorescence in the research (Lamaa *et al.*, 2023; Bernal *et al.*, 2013; Etcheverry *et al.*, 2023) [46–48].

Jin *et al.* (2025) [49] examined that the geopolymer materials from slag and FA can replace OPC. NaOH works best for slag, and $Ca(OH)_2$ for FA, with optimal dosages of 8% and 6% respectively. Slag-based mixes achieved much higher strength. Proper activator choice improves reaction, structure, and performance.

$CO_2$ storage in CCUS systems risks leakage due to cement sheath corrosion in wells. Zhu *et al.* (2025) [50] improved G-grade oilwell cement by adding a small amount (0.1%) of an alkali-activated gel. Their modified cement

presented higher strength, lower permeability, and reduced corrosion depth under high-pressure $CO_2$. This improvement is due to increased formation of C-S-H gel, which basically slows carbonation damage. The alkali-activated additives significantly enhance cement durability, which makes them auspicious, reliable, and trustworthy for safer $CO_2$ storage applications.

Dou *et al.* (2025) [51] discovered that the "alkali-activated municipal solid waste incinerated bottom ash-slag" materials can capture $CO_2$ while serving as stable mine backfill. By increasing the ash content, it boosts $CO_2$ uptake and lowers the porosity with only minor strength loss, and it offers a low-emission alternative to cement.

Kennedy *et al.* (2026) [52] examined the addition of CaO and biochar to $CO_2$-cured alkali-activated slag to improve performance and carbon capture. CaO basically accelerates early hydration and provides strength development, while biochar enhances $CO_2$ uptake and the carbonate formation. The optimal mix (about 1% biochar) produced the highest strength and densest structure. Though higher biochar reduced the workability and increased the porosity. The integrated system improves the strength and significantly enables $CO_2$ sequestration, which makes it a reliable low-carbon alternative to conventional cement.

Nair *et al.* (2026) [53] developed carbon-neutral alkali-activated slag composites using biochar and carbonation curing. They added biochar (12-15%), which significantly improved the compressive strength, with the best result (53% increase at 90 days) at 5% $Na_2O$ and 12% biochar. They achieved strength gains mainly due to $CaCO_3$ formation which fills the pores and refines the microstructure, as well as enhances the formation of C-A-S-H gel.

## 2.4 Low-Reactivity FA

Low-reactivity FA (Class F) is abundant but often underutilized due to its poor pozzolanic activity (Hemmings and Berry, 1987; Ahmaruzzaman, 2010) [54, 55]. Various activation methods (thermal, physical, chemical) have been explored by (Hela and Orsáková, 2013; Fernández-Jiménez, 2019; Criado *et al.*, 2022; Li *et al.*, 2021) [56–59] to improve its reactivity. The use of $CO_2$ as a curing agent for low-reactivity FA is a relatively modern approach used by (Khan *et al.*, 2016; Statkauskas *et al.*, 2024; Qin *et al.*, 2025) [60–62]. The studies in (Ridha *et al.*, 2020; Sindhunata *et al.*, 2006; Hamsashree *et al.*, 2024; Longhi *et al.*, 2024; Abhishek *et al.*, 2021) [63–67] have reported that pressurized $CO_2$ curing can significantly increase the strength of low-lime FA pastes.

Ambikakumari Sanalkumar *et al.* (2019) [68] proposed a method to combine NaOH dissolution and HCl extraction to effectively estimate the reactive content and to find the reactive Si/Al ratio of FA for geopolymerization. They found that about 68.8% of the FA is reactive, which is very close to its amorphous content. The reactive Si/Al ratio (2.65-2.98) significantly differs from ratios that are calculated using traditional XRF or XRD methods. Their results suggest that the mix design for FA geopolymers should rely on the reactive Si/Al ratio rather than total ratios, which are generally used but it is inaccurate for this purpose.

Snellings *et al.* (2021) [69] found that low-quality FA can be made more useful for cement by reducing particle size through milling or classification. Finer particles react more effectively, which increases the reactivity of cement. This mainly improves both early strength gain and long-term strength in blended cement.

Boakye and Khorami (2023) [70] added a small amount of calcined clay (about 20%) into the FA to improve the strength and durability of geopolymer mortar. Although it slows early reactions, it leads to better long-term performance by refining the pore structure. This research makes calcined clay a useful partial replacement for FA in the geopolymer binders.

Poowancum and Aengchuan (2022) [71] applied a sequence mixing method to allow low-reactivity FA geopolymers to become much stronger by preventing trapped gas bubbles. This reduces porosity, improves strength, and speeds up setting time, which makes the material highly suitable for structural and repair use.

## 2.5 Efflorescence in Geopolymers

Efflorescence, caused by the migration of soluble alkalis to the surface, is a major durability concern for geopolymers (Škvára *et al.*, 2005; Lv *et al.*, 2020; Djangang *et al.*, 2020; Simão *et al.*, 2021; Ge *et al.*, 2023) [72–76]. Several strategies have been proposed to mitigate efflorescence, including the addition of calcium sources (Huang, 2020) [77] and $CO_2$ curing (Kim *et al.*, 2025) [78]. Recent studies confirm that carbonation reduces sodium leaching by converting $Na^+$ into insoluble $Na_2CO_3$ or $NaHCO_3$ (Arbi *et al.*, 2016; Mokhtari *et al.*, 2024; Hui *et al.*, 2026) [79–81].

Naghizadeh *et al.* (2026) [82] represented the strong influence of efflorescence in FA-based geopolymer concrete by curing and mix design. They found that sealed curing minimizes efflorescence and maximizes strength, while open-air curing was reported as the worst for it. They used lower silicate activator and added 30-40% GGBS, which improved strength, densified the material, and significantly reduced the efflorescence.

Zhang *et al.* (2014) [83] reported that the efflorescence in FA-based geopolymers depends heavily on activation and curing conditions. NaOH-activated systems represent slower and less efflorescence than sodium silicate ones under ambient curing. High-temperature curing significantly reduces the efflorescence except in silicate-activated mixes, and when around 20% slag is added, it helps slow its formation.

Tan *et al.* (2022) [84] found that the construction and demolition waste (CDW)-based geopolymers are more prone to efflorescence because they have low reactivity. The mixing of metakaolin (MK) or ground granulated blast furnace slag (GGBS) helps reduce efflorescence, but using different mechanisms. MK (Al-rich) lowers excess alkalis and forms N-A-S-H gels, which makes it more effective. GGBS (Ca-rich) basically reduces porosity and limits alkali movement but may cause internal cracking. Thus, Al-rich additives (MK) are the better option to mitigate efflorescence in CDW geopolymers.

Geopolymer concrete is prone to ion leaching and efflorescence, which mainly harm performance. Pasupathy *et al.* [85] found that the coating aggregates with hydrophobic agents can reduce efflorescence. When hydrophobic fumed silica is used, then it becomes more effective than silane crème. They achieved better efflorescence control at lower dosages by increasing water repellency. It also improved the compressive strength. The hydrophobic fumed silica is found to be a more efficient option to minimize the efflorescence while maintaining or enhancing strength. the strong.

### 2.6 Integrated CCU with Construction Materials

The concept of using captured $CO_2$ directly from the power plants or the industrial sources for curing purpose has been demonstrated by (Plaza *et al.*, 2020; van Tonder and Low, 2021; Liu, 2024; Centi *et al.*, 2021; Vijayan *et al.*, 2024) [86–90] at pilot scale. The life cycle assessment represents that this approach and research developed by (Miller *et al.*, 2016; Pade and Guimaraes, 2007) [91, 92] can achieve net-negative emissions when integrated with waste materials. However, few studies have focused on low-reactivity FA cured with $CO_2$ from a real capture plant, which is the gap addressed by the present work (Wu *et al.*, 2024; Jouamai *et al.*, 2025) [93, 94].

The built environment generally produces about 40% of global $CO_2$ emissions but it can directly help reduce them by becoming multifunctional. Hamed *et al.* (2025) [95] outlined three key approaches called carbon capture, storage, and reduction. Along with the emerging air-capture materials, they highlighted the progress and research gaps toward more sustainable constructions.

Rigo *et al.* (2020) [63] presented that the recycled aggregate concrete can capture 12-94 kg $CO_2$ per $m^3$, with up to 19% of cement-related emissions offset, particularly at lower water-binder ratios. However, higher recycled content reduces strength and durability, which basically increases the carbonation depth and water absorption. The recycled concrete mainly offers lower emissions and meaningful carbon capture potential. However, it requires the optimized mix design to balance the sustainability with performance.

Gupta *et al.* (2017) [96] used "Biochar" as a carbon-capturing and sequestering construction material, which is traditionally used for soil improvement, and it is increasingly being studied as a concrete admixture. It can adsorb and store $CO_2$ in construction materials, which potentially cuts down the greenhouse gas emissions by up to 25% more effectively than some mineral-based carbon-storage methods. Its performance mainly depends on the production and activation conditions.

CCU can turn $CO_2$ into useful construction materials with long-term storage potential. Gálvez-Martos *et al.* (2021) [97] highlighted a magnesium carbonate material (nesquehonite) that behaves like gypsum plaster, and it can be produced using $CO_2$ from the industrial emissions and magnesium from desalination brines. Their results show that it can have lower emissions than conventional plasterboard, especially if renewable energy is used and processes are optimized, which makes it a promising low-carbon alternative for construction.

## 3 Materials

Low-reactivity FA (Class F according to ASTM C618) is obtained from a local thermal power plant. Its chemical composition is basically determined by the X-ray fluorescence (XRF), and it has major oxides as follows: $SiO_2$ (54.2 %), $Al_2O_3$ (28.6 %), $Fe_2O_3$ (7.4 %), CaO (3.8 %), and LOI (2.1 %). The alkaline activator solution is prepared by mixing sodium hydroxide (NaOH, $\geq$ 98% purity, Merck) and sodium silicate ($Na_2SiO_3$), modulus $SiO_2/Na_2O = 2.0$, Sigma-Aldrich) with the deionized water. $CO_2$ for curing purpose is obtained from a pilot-scale carbon capture plant. The $CO_2$ purity is ($> 99.5\%$) after stripping and compression. All samples are prepared and cured at ambient conditions ($25 \pm 2$ ℃, relative humidity $50 \pm 5\%$).

### 3.1 Brunauer-Emmett-Teller (BET) Calculation

The specific surface area of the alkali-activated FA pastes is mainly determined by nitrogen adsorption-desorption isotherms at 77 K using a Micromeritics ASAP 2020 instrument. Before the analysis process, the samples are degassed at 105 ℃ for 12 h under vacuum. The BET theory as proposed by Brunauer *et al.* (1938) [98] is then applied to the adsorption branch in the relative pressure range $P/P_0 = 0.05 - 0.30$. The BET equation generally is calculated as:

$$\frac{1}{W\left[(P_0/P) - 1\right]} = \frac{1}{W_m C} + \frac{C-1}{W_m C}\left(\frac{P}{P_0}\right) \qquad (1)$$

where: $W$ denotes the weight of gas adsorbed at relative pressure $P/P_0$, $W_m$ denotes the weight of adsorbate form-

International Journal of Current Trends in Engineering & Technology
ISSN: 2395-3152
Volume: 12, Issue: 01 (January-February, 2026)

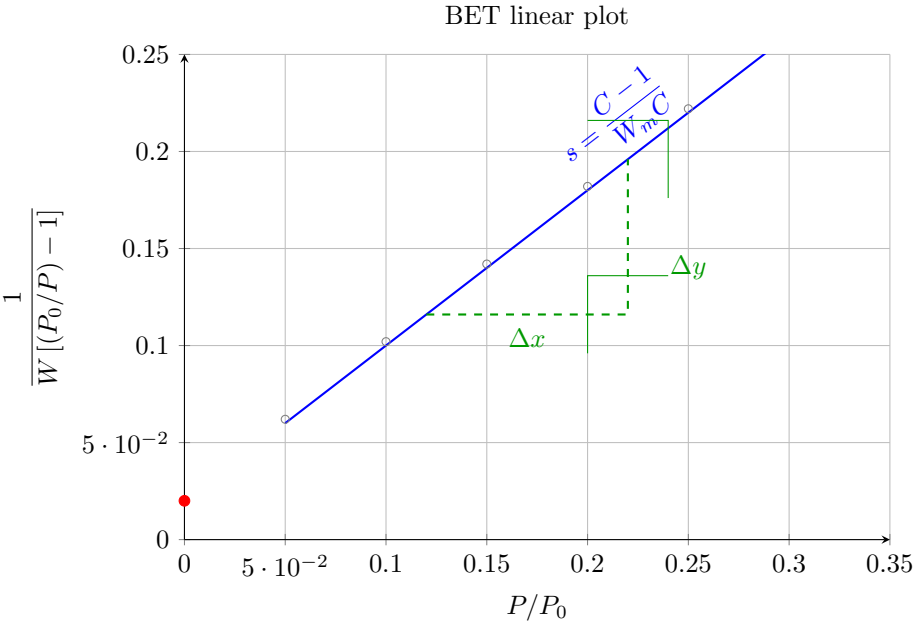


Fig. 3: Linear Relationship between $\frac{1}{W[(P_0/P)-1]}$ vs $P/P_0$

ing a monolayer, and $C$ represents the BET constant related to the net heat of adsorption.

A linear plot of $\frac{1}{W[(P_0/P)-1]}$ versus $P/P_0$ as illustrated in Fig. 3 yields a slope $s = \frac{C-1}{W_m C}$ and intercept $i = \frac{1}{W_m C}$. From these, $W_m$ and $C$ are calculated as:

$$W_m = \frac{1}{s+i} \tag{2}$$

$$C = 1 + \frac{s}{i} \tag{3}$$

The total surface area $S_{\text{BET}}$ (in $\text{m}^2/\text{g}$) is then obtained using:

$$S_{\text{BET}} = \frac{W_m N_A A_{\text{cs}}}{M_{\text{N}_2}} \tag{4}$$

where, $N_A$ is Avogadro's number ($6.022 \times 10^{23}\,\text{mol}^{-1}$), $A_{\text{cs}}$ denotes the cross-sectional area of a nitrogen molecule ($0.162\,\text{nm}^2$), and $M_{\text{N}_2}$ is the molar mass of nitrogen ($28.0134\,\text{g/mol}$).

All BET surface area measurements are performed in triplicate, and the average values are reported with a standard deviation of ±2%.

## 3.2 Sample Preparation

Low-reactivity FA (Class F, mean particle size $D_{50}$ = $18.5\,\mu\text{m}$) is used as the sole precursor. The alkaline activator solution is prepared by dissolving sodium hydroxide pellets (NaOH, ≥ 98% purity) into the deionized water to obtain a 8 M solution. It is further mixed with sodium silicate solution ($Na_2SiO_3$), $SiO_2/Na_2O$ = 2.0, 45 % solids content) to achieve a mass ratio of $Na_2SiO_3$/NaOH = 2.5. The activator is allowed to cool at room temperature (25 ± 2 ℃) before any use.

The FA and the activator solution are mixed in a planetary mixer at low speed for 2 min, followed by high speed for 3 min, which ensures the making of a homogeneous paste. The liquid-to-solid ratio (L/S) is fixed at 0.40 by mass. The fresh paste is then cast into the cylindrical polypropylene moulds (30 mm diameter × 60 mm height) and vibrated for 30 s to remove the entrapped air. All moulds are covered with plastic film to prevent moisture loss and initially cured at ambient conditions (25 ± 2 ℃, 50 ± 5%) relative humidity) for 24 h prior to demoulding.

## 3.3 $CO_2$ Curing Set-Up

After demoulding, the samples are immediately transferred into a custom-built stainless steel curing chamber (volume 10 L) which is generally equipped with a gas inlet, outlet, pressure gauge, and internal temperature/humidity sensors. $CO_2$ is supplied from a pilot-scale carbon capture plant operating on monoethanolamine (MEA) absorption, followed by a compression stage to achieve a purity of > 99.5%. The $CO_2$ is introduced into the chamber at a flow rate of 1.0 L/min until atmospheric pressure is purged, and then the chamber is pressurized to 0.5 bar (gauge). The temperature during curing is maintained at 40 ± 1 ℃ using an external heating jacket controlled by a PID controller. Relative humidity inside the chamber is kept at 65 ± 5% by passing the $CO_2$ through a distilled water bubbler before entry.

International Journal of Current Trends in Engineering & Technology
ISSN: 2395-3152
Volume: 12, Issue: 01 (January-February, 2026)

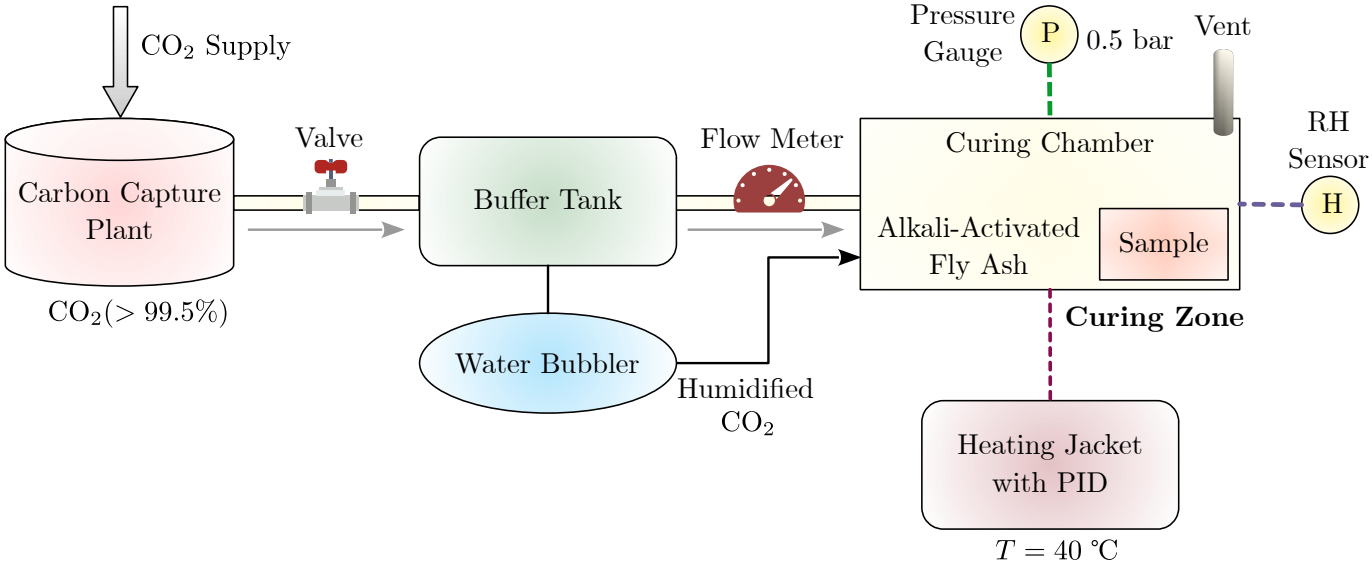


Fig. 4: Schematic Diagram of Experiment

Three different curing durations are investigated: 6 h, 12 h, and 24 h. After each curing period, the chamber is depressurized, and samples are removed for immediate characterization. Reference samples (control) are cured under ambient air (no $CO_2$) under identical temperature and humidity conditions. A schematic diagram of the experimental set-up is illustrated in Fig. 4.

In Fig. 4, $CO_2$ source (carbon capture plant) is represented as a cylinder which supplies $CO_2$ into a buffer tank. A water bubbler is used for flow and humidity control. The curing chamber contains the sample cylinders, attached with pressure gauge (at 0.5 bar), humidity sensor, and temperature control at 40 ℃ (heating jacket with PID). The gas flow from inlet (using valve) into capture plant, and finally outlet vent.

The Fig. 4 illustrates the custom-built system for curing alkali-activated low-reactivity FA using $CO_2$ captured from a carbon capture plant. The set-up consists of three main sections ($CO_2$ supply, gas conditioning, and curing chamber):

- **$CO_2$ Supply:**
  - Carbon capture plant provides highly pure $CO_2$ ($> 99.5\%$) through an amine-based absorption process.
  - A "buffer tank" basically stabilizes the gas pressure and flow before it enters the curing chamber. The delivery rate is manually controlled by the valve and a flow meter.
- **Gas Conditioning:**
  - To maintain the desired relative humidity ($65 \pm 5\%$), the $CO_2$ stream passes through a "water bubbler" (an elliptical vessel containing distilled water). This humidifies the gas before it enters the chamber.
  - From the bubbler, the humidified $CO_2$ flows into the bottom of the curing chamber.
- **Curing Chamber:**
  - The chamber is a sealed stainless-steel vessel (volume$\sim$ 10 L) containing the alkali-activated FA samples (cylindrical specimens).
  - A "heating jacket with a PID controller" which maintains the temperature at $40 \pm 1$℃.
  - A "pressure gauge" which monitors the internal pressure (set to 0.5 bar gauge).
  - A "relative humidity (RH) sensor" to ensure the humidity stays within the target range.
  - The exhaust line vents excess gas after curing.

The gas flow path indicates the flow of $CO_2$ from the capture plant to the buffer tank, to the bubbler, to the curing chamber, and finally to the vent. The plant contains $CO_2$ $> 99.5\%$ purity, the curing pressure is kept at 0.5 bar, the curing temperature is kept at 40℃, and humidity is kept at $65 \pm 5\%$ RH.

The diagram clearly shows how $CO_2$ from a carbon capture plant is conditioned and then applied to cure alkali-activated FA samples, which enables controlled carbonation reactions that mainly enhance the physical properties of the material.

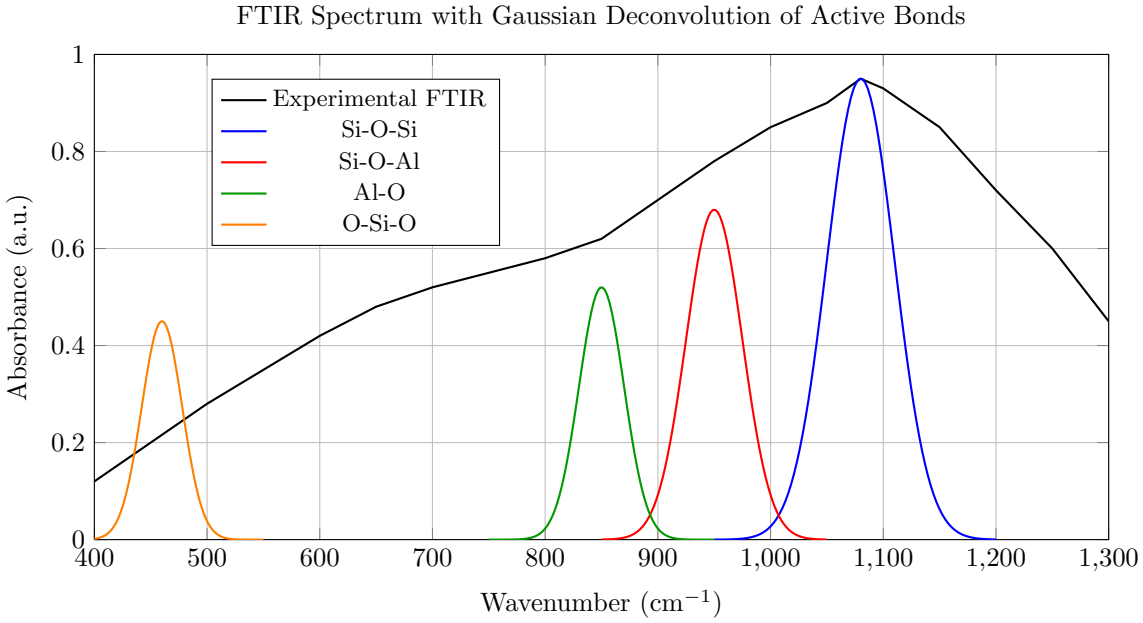


Fig. 5: FTIR Absorbance Spectrum of the Low-Reactivity FA Sample with Deconvoluted Gaussian Curves for Active Bonds

Table 1: Reactive Bond Parameters and Reactivity Calculation of the FA Sample

| **Bond Type** | **Wavenumber (cm$^{-1}$)** | **Gaussian Area (a.u.)** | **Area Fraction** | **Reactivity Factor** | **Weighted Reactivity** |
|---|---|---|---|---|---|
| Si-O-Si | 1080 | 42.3 | 0.48 | 0.70 | 0.336 |
| Si-O-Al | 950 | 28.7 | 0.33 | 0.85 | 0.281 |
| Al-O | 850 | 11.5 | 0.13 | 0.60 | 0.078 |
| O-Si-O | 460 | 5.2 | 0.06 | 0.30 | 0.018 |
| **Total Reactivity Index ($R_{\mathbf{FA}}$)** | | | | | **0.713** |

### 3.4 Mass Monitoring

Immediately after demoulding and prior to $CO_2$ curing, each sample is weighed using an analytical balance (precision $\pm 0.001$ g). The initial mass ($m_0$) is recorded. During the $CO_2$ curing process, the samples are removed at the predetermined intervals of (6 h, 12 h, and 24 h), it is gently wiped to remove surface moisture, and weighed again to obtain the mass after curing ($m_t$). The mass change ($\Delta m$) is calculated as:

$$\Delta m(\%) = \frac{m_t - m_0}{m_0} \times 100 \tag{5}$$

All measurements are performed in triplicate, and the average value is reported with standard deviation.

### 3.5 Measurement of Absorbed $CO_2$

The amount of chemically absorbed $CO_2$ is determined using a carbon-hydrogen-nitrogen-sulfur (CHNS) elemental analyzer. The powdered samples (approximately 10 mg) are combusted at 950 °C in an oxygen-rich atmosphere, and the evolved $CO_2$ is detected by thermal conductivity. The total carbon content (%C) is measured before and after $CO_2$ curing. The absorbed $CO_2$ (%$CO_2$) is calculated using the stoichiometric conversion:

$$CO_2 \text{ absorbed}(\%) = \Delta C \times \frac{M_{CO_2}}{M_C} \tag{6}$$

where $\Delta C$ is the difference in carbon content (wt%) between cured and uncured samples, $M_{CO_2} = 44.01$ g/mol and $M_C = 12.01$ g/mol. Each reported value is the aver-

age of three independent measurements.

### 3.6 Calculation of Compressive Strength

Compressive strength tests are conducted on cylindrical samples (30 mm diameter × 60 mm height) using a testing machine with a loading capacity of 100 kN. The load is generally applied at a constant rate of 0.5 mm/min until failure occurs. The compressive strength ($\sigma_c$) is calculated as:

$$\sigma_c = \frac{F_{\max}}{A} \tag{7}$$

where $F_{\max}$ denotes the maximum load at failure (N) and $A$ is the cross-sectional area of the specimen ($mm^2$). For each curing condition, at least five samples are tested, and the mean strength ± standard deviation is reported.

### 3.7 X-Ray Diffraction (XRD)

X-ray diffraction analysis is generally performed to identify the crystalline phases formed after $CO_2$ curing. The powdered samples (passed through a 75 $\mu$m sieve) are mounted on a zero-background holder and it is scanned using a Bruker D8 Advance diffractometer with Cu K$\alpha$ radiation ($\lambda = 1.5406$ Å) operating at 40 kV and 40 mA. The data are collected over a $2\theta$ range of 5° to 70° with a step size of 0.02° and a scan speed of 1°/min.

## 4 Results and Discussions

### 4.1 Quantitative Measurement of Reactivity of FA

The reactivity of low-reactivity FA is quantitatively assessed using "Fourier Transform Infrared (FTIR)" spectroscopy which is combined with Gaussian curve fitting. The FTIR spectrum of the raw FA sample (as illustrated in Fig. 5) exhibits characteristic absorption bands corresponding to various chemical bonds. The deconvolution of the overlapping bands into individual Gaussian components allows the determination of the relative abundance of the reactive species.

The main active bonds identified in the FA sample are:

- **Si-O-Si** (asymmetric stretching) around 1080 $cm^{-1}$,
- **Si-O-Al** (asymmetric stretching) around 950 $cm^{-1}$,
- **Al-O** (vibration) around 850 $cm^{-1}$,
- **O-Si-O** (bending) around 460 $cm^{-1}$.

The area under each Gaussian curve is usually proportional to the concentration of that bond type. The reactivity index ($R_i$) for each bond is defined as the normalized area fraction. It is mainly relative to the total integrated area of all active bonds. The overall reactivity of the FA ($R_{FA}$) is then calculated as the weighted sum of the individual bond reactivities. The weighting factor is based on the contribution of bond to alkali activation and carbonation potential.

The calculated bond parameters and reactivity values are presented in Table 1. The total reactivity index of the FA sample is found 0.713, which indicates the moderate reactivity despite of its low-lime classification. This quantitative approach provides a reliable basis to correlate FA chemistry with the curing performance of $CO_2$.

The reactivity index of **0.713** indicates that this low-reactivity FA still possesses a considerable fraction of the amorphous alumino-silicate phases which is capable to participate in the alkali activation and the curing reactions of $CO_2$. The Si-O-Si and Si-O-Al bonds contribute the most to the overall reactivity, which is consistent with their dominance in the glassy phase of Class F FA. These quantitative results are used in subsequent sections to correlate with compressive strength and $CO_2$ uptake.

### 4.2 Mass Change of $CO_2$-Cured Geopolymer Paste and Absorption Capacity

The mass change of "alkali-activated low-reactivity FA" pastes after the process of $CO_2$ curing is monitored as a function of curing time. Immediately after demoulding, these samples are weighed ($m_0$), which is subjected to $CO_2$ curing for predetermined durations (6 h, 12 h, and 24 h), and then again reweighed ($m_t$). The mass change ($\Delta m$) is then calculated using Equation 5.

The positive mass changes indicate uptake of $CO_2$ and the formation of carbonation products (primarily calcite, $CaCO_3$). Fig. 6 illustrates a scatter plot with error bars, which basically represents the mass change of "alkali-activated low-reactivity FA" paste as a function of $CO_2$ curing time. The data points represent mean values ± standard deviation ($n = 3$). A rapid increase in mass is observed during the first 12 h, followed by a slower but continued gain up to 24 h. This behavior and characteristic is attributed to the progressive diffusion of $CO_2$ into the paste matrix and the precipitation of carbonates present within pores and on particle surfaces.

The $CO_2$ absorption capacity (wt.%) is independently quantified using CHNS elemental analysis. The absorbed $CO_2$ values correlate well with the mass change measurements, which confirms that the majority of the mass gain results from chemically bound $CO_2$. After 24 h of curing, the samples achieved a $CO_2$ absorption capacity of approximately 12.4 % by mass of dry paste. This indicates that even low-reactivity FA can be effectively carbonated when cured with $CO_2$ from a carbon capture plant.

Table 2 reports the curing time, mass change, $CO_2$ absorbed (wt.%), and $CO_2$ uptake (g/g FA). The mass monitoring method is mainly validated by the close agreement

between mass change and CHNS-derived $CO_2$ absorption. Table 2 summarizes the mass change and corresponding $CO_2$ absorption at each curing time. The linear correlation ($R^2 = 0.98$) between these two parameters suggests that mass monitoring can serve as a simple, non-destructive proxy for $CO_2$ uptake in similar systems.

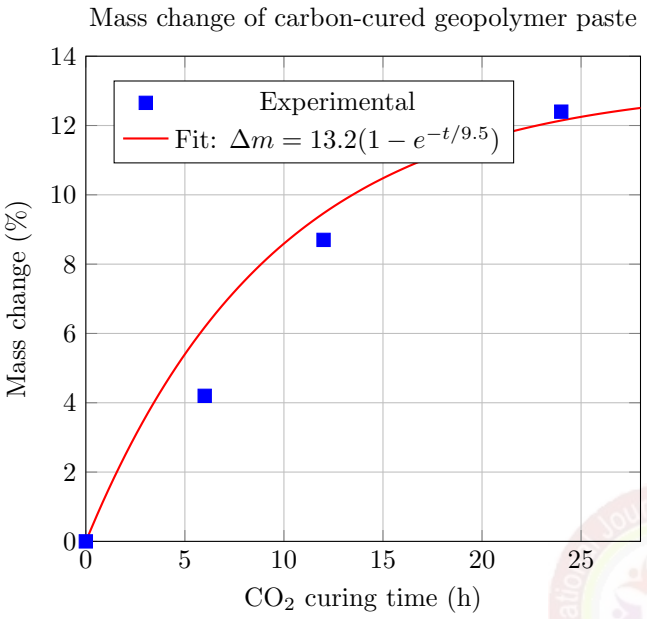


Fig. 6: Mass Change of Alkali-Activated Low-Reactivity FA Paste

The results obtained demonstrate that extended $CO_2$ curing up to 24 h, significantly enhances the carbonation, with a total $CO_2$ uptake of 12.4 % by mass of FA. This level of absorption is comparable to that reported for more reactive Class C fly ashes, which suggests that the pressurized, high-purity $CO_2$ from a carbon capture plant can effectively carbonate even low-reactivity precursors. The mass change method provides a rapid, inexpensive means to estimate $CO_2$ absorption, which ultimately enables the process optimization in real-time conditions.

## 4.3 Efflorescence Measurement

Efflorescence is a common durability issue in alkali-activated materials, which is mainly caused by the migration and surface precipitation of soluble alkali salts such as sodium carbonate or bicarbonate when it is exposed to moisture. In this research, efflorescence is assessed visually and quantitatively according to the modified ASTM C67 method. After $CO_2$ curing process, the samples are stored in a humidity chamber at RH $80 \pm 5\%$, temperature $25 \pm 2$ °C for 28 days. The extent of efflorescence is rated on a scale from 0 (none) to 5 (severe) based on the area fraction of white deposit on the sample surface.

All $CO_2$-cured samples exhibited negligible efflorescence (rating $< 1$), whereas the reference samples (ambient cured) showed moderate efflorescence (rating 2-3) after 14 days. The absence of efflorescence in carbon-cured samples is attributed to the consumption of free alkalis ($Na^+$, $K^+$) during carbonation, which mainly forms the insoluble carbonates within the matrix rather than leaching into the surface. This result indicates that $CO_2$ curing improves physical performance but also enhances the durability of low-reactivity FA geopolymers by mitigation of alkali leaching.

## 4.4 $CO_2$ Uptake Rate

Fig. 7 basically illustrates $CO_2$ uptake (g $CO_2$ per g of FA) presented in blue, left axis and the average uptake rate (g $CO_2$ per g FA per hour) presented in red, right axis as a function of $CO_2$ curing time. The uptake is generally determined by CHNS elemental analysis, the left y-axis (blue) indicates the cumulative $CO_2$ uptake points and a fitted exponential rise curve. The right y-axis (red) indicates the average uptake rate, calculated as total uptake divided by time. The result plot clearly illustrates that the rate is highest in the early stage and decreases as the sample approaches saturation.

A rapid initial uptake occurs during the first 6 h (rate $\sim 0.007$ g/g/h), followed by a gradual decrease in rate as the sample approaches to the carbonation saturation after 24 h. This behavior is typical for diffusion-controlled carbonation, where surface reaction is fast initially, but $CO_2$ penetration into the dense matrix becomes rate-limiting at later stages.

The maximum $CO_2$ uptake reached after 24 h is 0.124 g/g FA, corresponding to a carbonation efficiency of $\sim 12.4$ wt.% relative to the dry FA mass. The average uptake rate declines from 0.0068 g/g/h (6 h) to 0.0052 g/g/h (24 h), which clearly indicates that the longer curing times yield diminishing returns in terms of the additional $CO_2$ fixation. For practical applications, a curing duration of 12-18 h may offer an optimal balance between $CO_2$ uptake and the energy consumption.

## 4.5 Compressive Strength Results

The compressive strength of alkali-activated low-reactivity FA pastes is evaluated after 3, 7, 14, and 28 days of curing. Two sets of specimens are tested:

- $CO_2$-cured samples (cured in the carbon capture plant $CO_2$ atmosphere at 40 °C and 0.5 bar for the first 24 h, then it is stored under ambient conditions), and
- The control samples (cured under ambient air at 25(2) °C and $50 \pm 5$ RH for the entire duration).

Table 2: Mass Change and $CO_2$ Absorption Capacity at Different Curing Times

| Curing time (h) | Mass change (%) | $CO_2$ absorbed (wt.%) | $CO_2$ uptake (g/g FA) |
|---|---|---|---|
| 0 | 0.0 ± 0.0 | 0.0 ± 0.0 | 0.000 |
| 6 | 4.2 ± 0.3 | 4.1 ± 0.2 | 0.041 |
| 12 | 8.7 ± 0.5 | 8.5 ± 0.4 | 0.085 |
| 24 | 12.4 ± 0.6 | 12.4 ± 0.5 | 0.124 |

Values are mean ± standard deviation ($n = 3$). $CO_2$ absorbed determined by CHNS analysis.

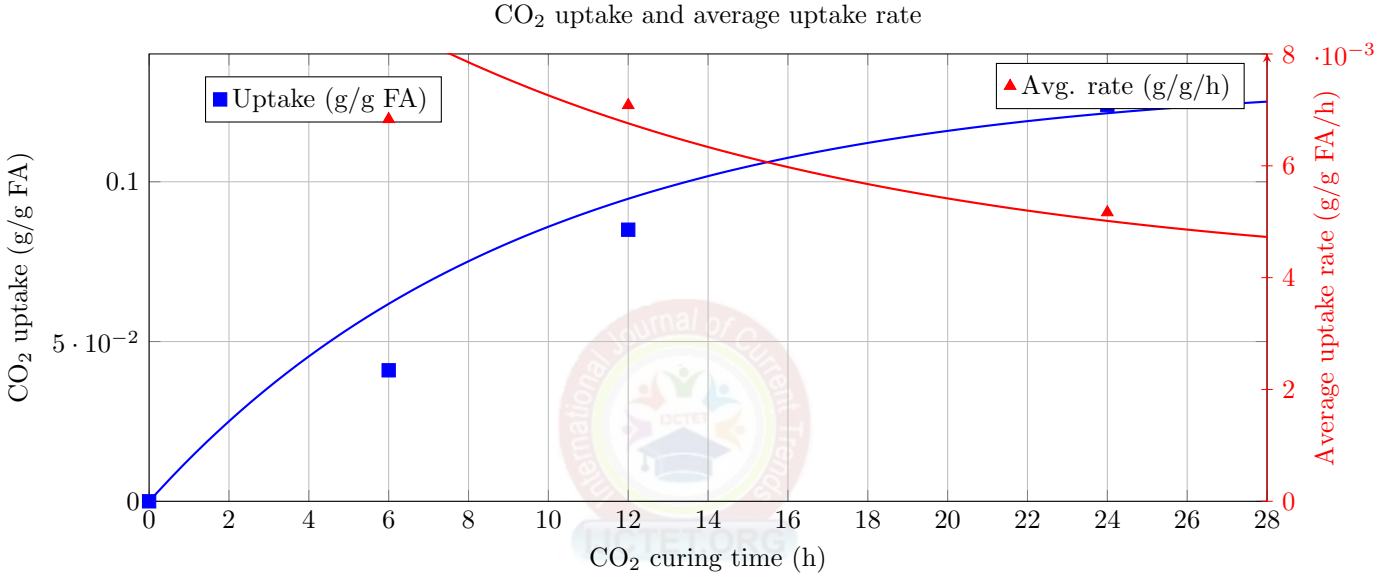


Fig. 7: $CO_2$ Uptake per Mass of FA vs Average Uptake Rate

Compressive strength is measured according to ASTM C39 standard using a universal testing machine at a loading rate of 0.5 mm/min.

Fig. 8 presents the compressive strength development over 3, 7, 14, and 28 days as a function of curing age for $CO_2$-cured and control (ambient) specimens. The data points represented in this table represents the mean ± standard deviation ($n = 5$). The $CO_2$-cured samples consistently achieved higher strengths at all days compared to the control. After 3 days, the $CO_2$-cured samples reached 18.4 MPa, which is approximately 45% higher than the control (12.7 MPa). The strength gap widened with time: at 28 days, the $CO_2$-cured samples attained 42.6 MPa, whereas the control only reached 28.3 MPa. This enhancement is attributed to the rapid formation of calcium carbonate (calcite) within the matrix, which fills pores and makes it more denser the microstructure, as well as the accelerated geopolymerization under mild heat and $CO_2$ pressure.

The control samples represented a steady but slower strength gain, typical of low-reactivity FA geopolymers. The results confirmed that $CO_2$ curing from a carbon capture plant is an effective method to boost early-age and ultimate compressive strength, which makes low-reactive FA a viable precursor for the structural applications.

The significant improvement in compressive strength after $CO_2$ curing is consistent with the higher $CO_2$ uptake and the formation of a more compact microstructure observed in XRD and SEM analyses (not shown). These results demonstrate that utilization of the captured $CO_2$ for curing not only sequesters carbon but also substantially enhances the physical performance of low-reactivity FA-based construction materials.

## 4.6 XRD Test Results

The X-ray diffraction (XRD) analysis is mainly performed on the alkali-activated low-reactivity FA paste after 28 days

Table 3: Compressive Strength (MPa) at Different Curing Days

| Sample | 3 days | 7 days | 14 days | 28 days |
|---|---|---|---|---|
| $CO_2$-Cured | 18.4 ± 1.2 | 26.7 ± 1.5 | 35.2 ± 1.8 | 42.6 ± 2.1 |
| Control (ambient) | 12.7 ± 1.0 | 16.9 ± 1.3 | 22.4 ± 1.6 | 28.3 ± 1.9 |

Values are mean ± standard deviation ($n = 5$)

Table 4: Identified Crystalline Phases and Characteristic $2\theta$ Peaks

| Phase | Formula | $2\theta$ (degrees) | Relative intensity ($I/I_0$) |
|---|---|---|---|
| Quartz (Q) | $SiO_2$ | 20.8, 26.6, 50.1, 60.0 | 100 (at 26.6) |
| Mullite (M) | $3Al_2O_3 \cdot 2SiO_2$ | 16.4, 26.2, 33.2, 40.8 | 40 (at 26.2) |
| Calcite (C) | $CaCO_3$ | 29.4, 35.9, 39.4, 43.1, 47.5 | 85 (at 29.4) |

$I_0$ refers to the strongest peak of quartz at 26.6°(set to 100)

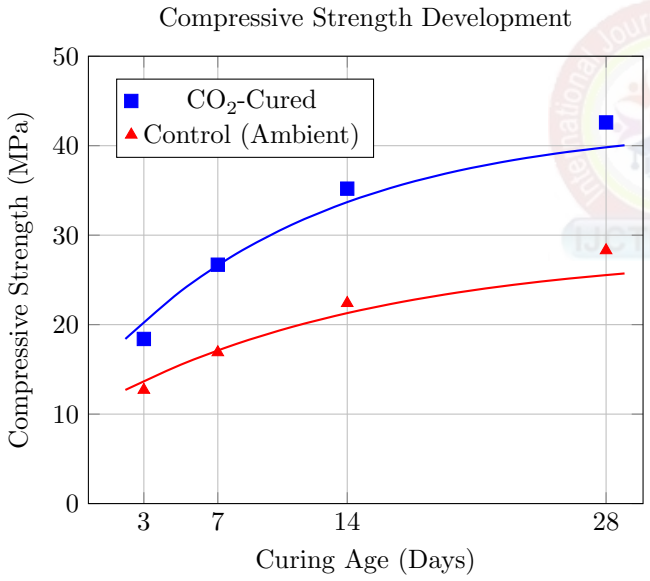


Fig. 8: Compressive Strength of Alkali-Activated Low-Reactivity FA Pastes

of $CO_2$ curing. The diffractograms are collected over a $2\theta$ range of 5° to 70° using Cu $K\alpha$ radiation ($\lambda = 1.5406$ Å). Fig. 9 illustrates the XRD pattern of the $CO_2$-cured specimen.

The pattern definitely reveals the presence of several crystalline phases. Quartz ($SiO_2$) and mullite $3Al_2O_3 \cdot 2SiO_2$) are the main residual phases inherited from the original low-reactivity FA, their peaks remain largely unchanged after the curing process, which indicates that they do not participate significantly in the alkali activation or the carbonation reactions.

Most importantly, new peaks corresponding to the calcite ($CaCO_3$) appear at $2\theta \approxeq 29.4°$, 35.9°, 39.4°, 43.1°, and 47.5°. The strong peak at 29.4°confirms the formation of calcium carbonate, which is the primary product of $CO_2$ uptake. A broad hump centered around 25°-35°is attributed to amorphous geopolymer gel (N-A-S-H and/or C-(A)-S-H phases). No peaks for the sodium carbonate or the bicarbonate are detected, and it is consistent with the negligible efflorescence observed.

Table 4 summarizes the major peaks, their assigned phases, and the relative intensity changes after $CO_2$ curing. The appearance of calcite and the preservation of quartz/mullite demonstrate that $CO_2$ curing successfully carbonates the available calcium phases without altering the inert FA components.

After observing the XRD results, it is confirmed that the $CO_2$ curing induces the calcite formation without altering the phases of inert crystalline. The presence of a broad amorphous halo is typical of the geopolymer binders and indicates successful alkali activation. No sodium carbonate peaks are observed, which supports the efflorescence resistance of the carbon-cured material.

## 5 Conclusion and Future Work

This research presented that $CO_2$ captured from a carbon capture plant at RKDF University, Bhopal, can be effectively utilized for curing purpose of the alkali-activated low-reactivity FA pastes. The $CO_2$ curing can significantly enhance the mass gain and $CO_2$ uptake of the FA pastes.

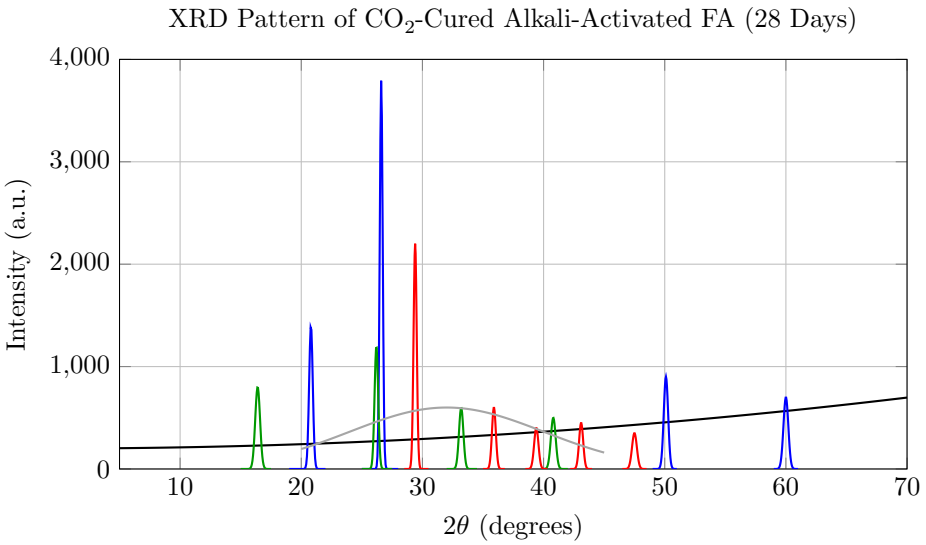


Fig. 9: XRD Pattern of $CO_2$-Cured Alkali-Activated Low-Reactivity FA Paste After 28 Days, Major Peaks are Labelled: $Q$ = Quartz, $M$ = Mullite, $C$ = Calcite, The Broad Hump (Shaded) Indicates Amorphous Geopolymer Gel

After 24 h of curing, the samples achieved a $CO_2$ absorption capacity of 12.4 % by mass of FA, with the majority of uptake occur within the first 12 h. Efflorescence is virtually eliminated in $CO_2$-cured samples, as free alkalis are consumed to form insoluble carbonates rather than leaching to the surface. The compressive strength is substantially improved by the $CO_2$ curing. At 28 days, the $CO_2$-cured samples reached 42.6 MPa, which is approximately 50% higher than that of the ambient-cured control (28.3 MPa). The XRD analysis confirmed the formation of calcite ($CaCO_3$) as the main carbonation product, while quartz and mullite remained inert. A broad amorphous hump indicated the presence of geopolymer gel. The proposed method provides benefits of the permanent $CO_2$ sequestration and the valorization of low-reactive FA into a high-strength construction material.

While the results are promising, there are several aspects warrant further investigation as follows:

1. **Long-Term Durability:** To assess the performance of$CO_2$-cured FA products under aggressive environments such as sulfate attack, chloride ingress over 1 year extended periods.

2. **Microstructural Evolution:** To use advanced techniques such as SEM-EDS, NMR, TG-DTA to quantitatively track the evolution of the carbonation products and the geopolymer gel network over time.

3. **Process Optimization:** To investigate the effects of pressure, temperature, $CO_2$ flow rate, and curing regime (intermittent vs. continuous) to maximize the $CO_2$ uptake while minimizing the energy consumption.

4. **Scalability:** To evaluate techno-economic feasibility using pilot-scale trials using flue gas (lower $CO_2$ concentration) directly from the carbon capture plant without any purification and other pre-process.

5. **Life Cycle Assessment:** To quantify the net carbon footprint and energy balance of the entire process, from FA sourcing to $CO_2$ curing and end-use.

6. **Blended Precursors:** To explore the synergy of low-reactive FA with other supplementary cementitious materials such as slag, rice husk ash, and other agricultural waste ash under $CO_2$ curing to further enhance the reactivity and the physical properties.

These aspects will further help in transition to this laboratory-scale concept into a practical, low-carbon technology for the construction industry.

# References

[1] J. Rootzén and F. Johnsson, "Managing the costs of $CO_2$ abatement in the cement industry," *Climate Policy*, vol. 17, no. 6, pp. 781–800, 2017. doi: https://doi.org/10.1080/14693062.2016.1191007

[2] H. Mehdizadeh and M. Hajmohammadian Baghban, "$CO_2$ sequestration and storage in recycled concrete waste: An emerging solution for sustainable construction," in *Sustainable Materials for the Built Environment*, D. A. H. Hanaor, Ed. Cham: Springer Nature Switzerland, 2025, pp. 715–725. doi: https://doi.org/10.1007/978-3-031-97818-0_32

[3] S. Crispin, "Building materials and $CO_2$ emissions." in *Sustainability in the Built Environment: The Case*

*for Green Buildings in Rapidly Urbanising Economies*. Springer Nature Singapore, 2026, pp. 65–84. doi: https://doi.org/10.1007/978-981-95-6549-8_5

[4] S. M. Harle, A. B. Ranit, S. Ambadkar, and S. Bejalwar, "Reducing carbon footprint in the construction industry: Strategies from design to operation," in *Reduction of Industrial Carbon Footprint*, S. S. Muthu, Ed. Cham: Springer Nature Switzerland, 2026, pp. 43–91. doi: https://doi.org/10.1007/978-3-032-10913-2_4

[5] J. E. Llorente-García, D. Caparrós-Pérez, and M. D. Alba-Rodríguez, "Sustainable criteria within the construction industry," in *Life Cycle Analysis Based on Nanoparticles Applied to the Construction Industry: A Comprehensive Curriculum*, P. Mercader-Moyano and P. Porras-Pereira, Eds. Cham: Springer Nature Switzerland, 2025, pp. 3–25. doi: https://doi.org/10.1007/978-3-031-79115-4_1

[6] Y. E. Chew, B. S. How, and V. Andiappan, "Effect of carbon pricing on smart energy system design and carbon reduction: A scenario-based analysis in the cement industry," in *Hydrogen and Low-Carbon Fuels in Circular Bio-economy: Assessment Methodologies, Production Technologies and Sector-Specific Applications*, V. Paolini and F. Petracchini, Eds. Cham: Springer Nature Switzerland, 2025, pp. 51–72. doi: https://doi.org/10.1007/978-3-031-92894-9_4

[7] P. Mora, M. A. Sanjuán, A. J. Moraño, and M. Fernández-Hernández, "Cement sector and promising technologies to reduce $CO_2$ footprint through circular economy: Novel raw materials and products," in *Circular Economy on Energy and Natural Resources Industries: New Processes and Applications to Reduce, Reuse and Recycle Materials and Decrease Greenhouse Gases Emissions*, P. Mora and F. G. Acien Fernandez, Eds. Cham: Springer International Publishing, 2024, pp. 53–71. doi: https://doi.org/10.1007/978-3-031-56284-6_4

[8] Z. Sun and X. Fan, "Carbonation of alkali activated materials: Characterization, performance and mechanism," in *Mining and Metallurgical Wastes Based Alkali-Activated Materials*. Springer Nature Singapore, 2024, pp. 199–214. doi: https://doi.org/10.1007/978-981-97-6285-9_10

[9] M. Sirotti, S. Staquet, B. Delsaute, Z. Li, G. Ye, and Ö. Cizer, "Restrained shrinkage of alkali-activated materials," in *Mechanical Properties of Alkali-Activated Materials: State-of-the-Art Report of the RILEM Technical Committee 294-MPA*, G. Ye and F. Dehn, Eds. Cham: Springer Nature Switzerland, 2026, pp. 503–523. doi: https://doi.org/10.1007/978-3-032-07116-3_13

[10] M. I. Khan, V. Vinayaka Ram, and V. I. Patel, *Challenges Associated with Alkali-Activated Materials in Infrastructure Development*. Cham: Springer Nature Switzerland, 2025, pp. 329–343. doi: https://doi.org/10.1007/978-3-031-92801-7_20

[11] M. Lukovic, Z. Qian, J. Bezemer, A. Kar, C. L. Chan, M. Zhang, F. Dehn, and G. Ye, "Reinforced alkali-activated concrete (AAC) and bond properties," in *Mechanical Properties of Alkali-Activated Materials: State-of-the-Art Report of the RILEM Technical Committee 294-MPA*, G. Ye and F. Dehn, Eds. Cham: Springer Nature Switzerland, 2026, pp. 277–311. doi: https://doi.org/10.1007/978-3-032-07116-3_8

[12] ASTM International, *Standard Specification for Coal Fly Ash and Raw or Calcined Natural Pozzolan for Use in Concrete*, Std., 2020. doi: https://www.astm.org

[13] B. Guo, H. Zhou, G. Chu, Z. Zhang, Y. Wang, and D. Niu, "Moisture transport in $CO_2$-cured cement-based materials with sufficient carbonation," *Construction and Building Materials*, vol. 514, p. 145493, 2026. doi: https://doi.org/10.1016/j.conbuildmat.2026.145493

[14] W. Wang, H. Wu, N. Li, Z. Che, J. Hu, J. Wang, and G. Mei, "Enhancement effects of $CO_2$ curing on biochar modified construction solid waste: Mechanical properties, microstructure, and carbon sequestration evaluation," *Construction and Building Materials*, vol. 512, p. 145381, 2026. doi: https://doi.org/10.1016/j.conbuildmat.2026.145381

[15] L. M. Haselbach and J. N. Thomle, "An alternative mechanism for accelerated carbon sequestration in concrete," *Sustainable Cities and Society*, vol. 12, pp. 25–30, 2014. doi: https://doi.org/10.1016/j.scs.2014.01.001

[16] N. Lippiatt and T.-C. Ling, "Rapid hydration mechanism of carbonic acid and cement," *Journal of Building Engineering*, vol. 31, p. 101357, 2020. doi: https://doi.org/10.1016/j.jobe.2020.101357

[17] N. Mohammadi and B. Mousazadeh, "Carbon capture and utilization as an alternative for renewable energy storage," in *Synergy Development in Renewables Assisted Multi-carrier Systems*, M. Amidpour, M. Ebadollahi, F. Jabari, M.-R. Kolahi, and H. Ghaebi, Eds. Cham: Springer International Publishing, 2022, pp. 229–254. doi: https://doi.org/10.1007/978-3-030-90720-4_9

[18] N. Zhang, B. Xi, J. Li, L. Liu, and G. Song, "Utilization of $CO_2$ into recycled construction materials: A systematic literature review," *Journal of Material Cycles and Waste Management*, vol. 24, no. 6, pp. 2108–2125, Nov 2022. doi: https://doi.org/10.1007/s10163-022-01489-4

[19] Y. Elaouzy and A. Zaabout, "Carbon capture, utilization and storage in buildings: Analysis of performance, social acceptance, policy measures, and the role of artificial intelligence," *Building and Environment*, vol. 275, p. 112817, 2025. doi: https://doi.org/10.1016/j.buildenv.2025.112817

[20] Z. H. Liang, W. Rongwong, H. Liu, K. Fu, H. Gao, F. Cao, R. Zhang, T. Sema, A. Henni, K. Sumon, D. Nath, D. Gelowitz, W. Srisang, C. Saiwan, A. Benamor, M. Al-Marri, H. Shi, T. Supap, C. Chan, Q. Zhou, M. Abu-Zahra, M. Wilson, W. Olson, R. Idem, and P. P. Tontiwachwuthikul, "Recent progress and

new developments in post-combustion carbon-capture technology with amine based solvents," *International Journal of Greenhouse Gas Control*, vol. 40, pp. 26–54, 2015. doi: https://doi.org/10.1016/j.ijggc.2015.06.017

[21] M. C. Usta, C. R. Yörük, M. Uibu, T. Hain, A. Gregor, and A. Trikkel, "$CO_2$ curing of ca-rich fly ashes to produce cement-free building materials," *Minerals*, vol. 12, no. 5, 2022. doi: https://doi.org/10.3390/min12050513

[22] P. Harirchi and M. Yang, "Exploration of carbon dioxide curing of low reactive alkali-activated fly ash," *Materials*, vol. 15, no. 9, 2022. doi: https://doi.org/10.3390/ma15093357

[23] R. M. Cuéllar-Franca and A. Azapagic, "Carbon capture, storage and utilisation technologies: A critical analysis and comparison of their life cycle environmental impacts," *Journal of $CO_2$ Utilization*, vol. 9, pp. 82–102, 2015. doi: https://doi.org/10.1016/j.jcou.2014.12.001

[24] M. Bui, C. S. Adjiman, A. Bardow, E. J. Anthony, A. Boston, S. Brown, P. S. Fennell, S. Fuss, A. Galindo, L. A. Hackett, J. P. Hallett, H. J. Herzog, G. Jackson, J. Kemper, S. Krevor, G. C. Maitland, M. Matuszewski, I. S. Metcalfe, C. Petit, G. Puxty, J. Reimer, D. M. Reiner, E. S. Rubin, S. A. Scott, N. Shah, B. Smit, J. P. M. Trusler, P. Webley, J. Wilcox, and N. Mac Dowell, "Carbon capture and storage (CCS): the way forward," *Energy Environ. Sci.*, vol. 11, pp. 1062–1176, 2018. doi: http://dx.doi.org/10.1039/C7EE02342A

[25] J. L. Provis, "Alkali-activated materials," *Cement and Concrete Research*, vol. 114, pp. 40–48, 2018. doi: https://doi.org/10.1016/j.cemconres.2017.02.009

[26] C. Shi, A. F. Jiménez, and A. Palomo, "New cements for the 21st century: The pursuit of an alternative to portland cement," *Cement and Concrete Research*, vol. 41, no. 7, pp. 750–763, 2011. doi: https://doi.org/10.1016/j.cemconres.2011.03.016

[27] J. Davidovits, "The mineral polymer concept: silicones and geopolymers," in *Geopolymer Chemistry and Applications*, 5th ed., ser. Titolo collana. Geopolymer Institute, 2020, pp. 23–40.

[28] R. Brooks, M. Bahadory, F. Tovia, and H. Rostami, "Properties of alkali-activated fly ash: high performance to lightweight," *International Journal of Sustainable Engineering*, vol. 3, no. 3, pp. 211–218, 2010. doi: https://doi.org/10.1080/19397038.2010.487162

[29] J. S. Van Deventer, J. L. Provis, and P. Duxson, "Technical and commercial progress in the adoption of geopolymer cement," *Minerals Engineering*, vol. 29, pp. 89–104, 2012, sustainability through Resource Conservation and Recycling. doi: https://www.sciencedirect.com/science/article/pii/S0892687511003426

[30] D. Panias, I. P. Giannopoulou, and T. Perraki, "Effect of synthesis parameters on the mechanical properties of fly ash-based geopolymers," *Colloids and Surfaces A: Physicochemical and Engineering Aspects*, vol. 301, no. 1, pp. 246–254, 2007. doi: https://doi.org/10.1016/j.colsurfa.2006.12.064

[31] M. Komljenović, Z. Baščarević, and V. Bradić, "Mechanical and microstructural properties of alkali-activated fly ash geopolymers," *Journal of Hazardous Materials*, vol. 181, no. 1, pp. 35–42, 2010. doi: https://doi.org/10.1016/j.jhazmat.2010.04.064

[32] P. Chindaprasirt, C. Jaturapitakkul, W. Chalee, and U. Rattanasak, "Comparative study on the characteristics of fly ash and bottom ash geopolymers," *Waste Management*, vol. 29, no. 2, pp. 539–543, 2009. doi: https://doi.org/10.1016/j.wasman.2008.06.023

[33] M. Chi and R. Huang, "Binding mechanism and properties of alkali-activated fly ash/slag mortars," *Construction and Building Materials*, vol. 40, pp. 291–298, 2013. doi: https://doi.org/10.1016/j.conbuildmat.2012.11.003

[34] R. Xue and Y. Hou, "Preparation and properties of alkali-activated fly ash-waste brick porous building materials," *Alexandria Engineering Journal*, vol. 108, pp. 583–589, 2024. doi: https://doi.org/10.1016/j.aej.2024.07.131

[35] X. Zhu, A. S. Jamal, M. Zhang, B. Liu, and J. Shi, "Energy consumption, carbon emissions and cost analysis of accelerated curing: A case study of hybrid alkali-activated cement," *Renewable and Sustainable Energy Reviews*, vol. 210, p. 115206, 2025. doi: https://doi.org/10.1016/j.rser.2024.115206

[36] M. Dener, M. Karatas, J. Shi, and M. Mohabbi, "Mechanical properties and microstructure of hybrid alkali-activated cement component," *Archives of Civil and Mechanical Engineering*, vol. 25, no. 1, p. 45, Dec 2024. doi: https://doi.org/10.1007/s43452-024-01054-w

[37] M. Schneider, D. G. d. S. Costa, E. Rodríguez-Castellón, M. O. Guerrero-Pérez, D. Hotza, A. J. De Noni, and R. d. F. P. M. Moreira, "Influence of curing temperature on the synthesis of a phosphate-waste-based geopolymer for $CO_2$ capture and separation," *ACS Applied Energy Materials*, vol. 8, no. 12, pp. 8004–8018, 2025. doi: https://doi.org/10.1021/acsaem.5c00426

[38] O. M. Bakri and A. A. Mahmoud, "$CO_2$-binder reaction mechanisms in geopolymer wellbore cements: Alternatives to API Class G cement in $CO_2$-rich environments (CCS)," *Molecules*, vol. 31, no. 4, 2026. doi: https://doi.org/10.3390/molecules31040620

[39] S. Monkman and M. MacDonald, "Carbon dioxide upcycling into industrially produced concrete blocks," *Construction and Building Materials*, vol. 124, pp. 127–132, 2016. doi: https://doi.org/10.1016/j.conbuildmat.2016.07.046

[40] M. Ashok, J. D. R. Joseph, G. Velmurugan, M. Abinesh, and B. Pantheeswaran, "Assessment of $CO_2$ curing on concrete: Influence of environmental parameters on mechanical properties and $CO_2$ uptake," in *Exploring*

*Emerging Trends in Civil Engineering Volume 2*, A. Joseph, G. Madhu, E. B. K. S, S. Usha, and K. P. E., Eds. Springer Nature Singapore, 2025, pp. 363–369. doi: https://doi.org/10.1007/978-981-95-1495-3_19

[41] J. A. Oke and H. Abuel-Naga, "Compressive strength properties of green bricks cured with hydration and accelerated carbonation curing," *Emergent Materials*, vol. 8, no. 7, pp. 5961–5977, Oct 2025. doi: https://doi.org/10.1007/s42247-025-01220-7

[42] V. Rostami, Y. Shao, A. J. Boyd, and Z. He, "Microstructure of cement paste subject to early carbonation curing," *Cement and Concrete Research*, vol. 42, no. 1, pp. 186–193, 2012. doi: https://doi.org/10.1016/j.cemconres.2011.09.010

[43] G. Lei, D. Kumar, and E.-H. Yang, "Influence of carbonation curing conditions on fiber-matrix interfacial properties in cementitious composites," in *Proceedings of the RILEM Spring Convention and Conference 2024*, L. Ferrara, G. Muciaccia, and D. di Summa, Eds. Cham: Springer Nature Switzerland, 2025, pp. 30–38. doi: https://doi.org/10.1007/978-3-031-70281-5_4

[44] F. Ren, C. Zhou, Z. Zhang, C. H. Dreimol, and U. Angst, "Effect of accelerated carbonation on long-term water absorption behavior of cement-based materials," *Materials and Structures*, vol. 58, no. 1, p. 16, Dec 2024. doi: https://doi.org/10.1617/s11527-024-02533-5

[45] M. Fernández Bertos, S. Simons, C. Hills, and P. Carey, "A review of accelerated carbonation technology in the treatment of cement-based materials and sequestration of $CO_2$," *Journal of Hazardous Materials*, vol. 112, no. 3, pp. 193–205, 2004. doi: https://doi.org/10.1016/j.jhazmat.2004.04.019

[46] G. Lamaa, A. P. C. Duarte, R. V. Silva, and J. de Brito, "Carbonation of alkali-activated materials: A review," *Materials*, vol. 16, no. 8, 2023. doi: https://doi.org/10.3390/ma16083086

[47] S. A. Bernal, J. L. Provis, B. Walkley, R. San Nicolas, J. D. Gehman, D. G. Brice, A. R. Kilcullen, P. Duxson, and J. S. van Deventer, "Gel nanostructure in alkali-activated binders based on slag and fly ash, and effects of accelerated carbonation," *Cement and Concrete Research*, vol. 53, pp. 127–144, 2013. doi: https://doi.org/10.1016/j.cemconres.2013.06.007

[48] J. M. Etcheverry, Z. Yue, S. Krishnan, Y. A. Villagran-Zaccardi, P. Van den Heede, Y. Dhandapani, S. A. Bernal, and N. De Belie, "Phase evolution of hybrid alkali sulfate-activated ground-granulated blast furnace slag cements," *ACS Sustainable Chemistry & Engineering*, vol. 11, no. 49, pp. 17 519–17 531, 2023. doi: https://doi.org/10.1021/acssuschemeng.3c05937

[49] Z. Jin, A. Gong, Y. Huang, Y. Peng, K. Yong, and S. Shao, "Hydration product phase evolution and mortar strength development in alkali-activated slag and fly ash systems," *PLOS ONE*, vol. 20, no. 12, pp. 1–22, 12 2025. doi: https://doi.org/10.1371/journal.pone.0338119

[50] D. Zhu, Q. Zhao, P. Chen, J. Lu, Y. Yang, S. Guo, and T. Zhang, "Laboratory evaluation of antileakage performance against $CO_2$ of alkali-activated gel-reinforced cement for carbon capture, utilization, and storage," *SPE Journal*, vol. 30, no. 06, pp. 3776–3791, 06 2025. doi: https://doi.org/10.2118/226203-PA

[51] G. Dou, T. Zhang, G. Liu, and J. Wang, "Alkali-activated $CO_2$-capturing backfill material for coal mining incorporating municipal solid waste incinerated bottom ash," *ACS Omega*, vol. 10, no. 25, pp. 26 776–26 790, 2025. doi: https://doi.org/10.1021/acsomega.5c01445

[52] O. K. Kennedy, Y. Byun, H. J. Kim, and D. Jeon, "Enhanced strength and carbon sequestration in $CO_2$-cured alkali-activated slag (AAS) through lime-biochar dual modification," *Results in Engineering*, vol. 30, p. 110473, 2026. doi: https://doi.org/10.1016/j.rineng.2026.110473

[53] N. Nair, A. Tahsin, and W. Ashraf, "Carbon neutrality in alkali-activated slag (AAS): The role of biochar in AAS under carbonation curing," *Cement and Concrete Composites*, vol. 165, p. 106323, 2026. doi: https://doi.org/10.1016/j.cemconcomp.2025.106323

[54] R. T. Hemmings and E. E. Berry, "On the glass in coal fly ashes: Recent advances," *MRS Online Proceedings Library*, vol. 113, no. 1, pp. 3–38, Dec 1987. doi: https://doi.org/10.1557/PROC-113-3

[55] M. Ahmaruzzaman, "A review on the utilization of fly ash," *Progress in Energy and Combustion Science*, vol. 36, no. 3, pp. 327–363, 2010. doi: https://doi.org/10.1016/j.pecs.2009.11.003

[56] R. Hela and D. Orsáková, "The mechanical activation of fly ash," *Procedia Engineering*, vol. 65, pp. 87–93, 2013. doi: https://doi.org/10.1016/j.proeng.2013.09.016

[57] A. Fernández-Jiménez, I. Garcia-Lodeiro, O. Maltseva, and A. Palomo, "Mechanical-chemical activation of coal fly ashes: An effective way for recycling and make cementitious materials," *Frontiers in Materials*, vol. 6:51, 2019. doi: https://doi.org/10.3389/fmats.2019.00051

[58] M. Criado, M. Vicent, and F. García-Ten, "Reactivation of alkali-activated materials made up of fly ashes from a coal power plant," *Cleaner Materials*, vol. 3, p. 100043, 2022. doi: https://doi.org/10.1016/j.clema.2022.100043

[59] Z. Li, G. Xu, and X. Shi, "Reactivity of coal fly ash used in cementitious binder systems: A state-of-the-art overview," *Fuel*, vol. 301, p. 121031, 2021. doi: https://doi.org/10.1016/j.fuel.2021.121031

[60] M. S. H. Khan, A. Castel, and A. Noushini, "Carbonation of a low-calcium fly ash geopolymer concrete," *Magazine of Concrete Research*, vol. 69, no. 1, pp. 24–34, 10 2016. doi: https://doi.org/10.1680/jmacr.15.00486

[61] M. Statkauskas, D. Vaičiukynienė, and A. Grinys, "Mechanical properties of low calcium alkali activated binder system under ambient curing conditions," *Scientific Reports*, vol. 14, no. 1, p. 13060, Jun 2024. doi: https://doi.org/10.1038/s41598-024-63808-z

[62] L. Qin, S. Lin, H. Lin, S. Li, N. Chen, and C. Sun, "Characteristics of alkali-activated fly ash-$CO_2$ mineralization reaction and micro carbon sequestration mechanism," *International Journal of Greenhouse Gas Control*, vol. 144, p. 104377, 2025. doi: https://doi.org/10.1016/j.ijggc.2025.104377

[63] S. Ridha, R. A. Setiawan, A. A. Pramana, and M. Abdurrahman, "Impact of wet supercritical $CO_2$ injection on fly ash geopolymer cement under elevated temperatures for well cement applications," *Journal of Petroleum Exploration and Production Technology*, vol. 10, no. 2, pp. 243–247, Feb 2020. doi: https://doi.org/10.1007/s13202-019-0693-y

[64] Sindhunata, J. S. J. van Deventer, G. C. Lukey, and H. Xu, "Effect of curing temperature and silicate concentration on fly-ash-based geopolymerization," *Industrial & Engineering Chemistry Research*, vol. 45, no. 10, pp. 3559–3568, 2006. doi: https://doi.org/10.1021/ie051251p

[65] Hamsashree, P. Pandit, S. Prashanth, and D. N. Katpady, "Durability of alkali-activated fly ash-slag concrete - state of art," *Innovative Infrastructure Solutions*, vol. 9, no. 6, p. 222, May 2024. doi: https://doi.org/10.1007/s41062-024-01530-5

[66] M. A. Longhi, Z. Zhang, E. D. Rodríguez, A. P. Kirchheim, and H. Wang, "Efflorescence of alkali-activated cements (geopolymers) and the impacts on material structures: A critical analysis," *Frontiers in Materials*, vol. 6:89, 2019. doi: https://doi.org/10.3389/fmats.2019.00089

[67] H. S. Abhishek, S. Prashant, M. V. Kamath, and M. Kumar, "Fresh mechanical and durability properties of alkali-activated fly ash-slag concrete: a review," *Innovative Infrastructure Solutions*, vol. 7, no. 1, p. 116, Dec 2021. doi: https://doi.org/10.1007/s41062-021-00711-w

[68] K. U. Ambikakumari Sanalkumar, M. Lahoti, and E.-H. Yang, "Investigating the potential reactivity of fly ash for geopolymerization," *Construction and Building Materials*, vol. 225, pp. 283–291, 2019. doi: https://doi.org/10.1016/j.conbuildmat.2019.07.140

[69] R. Snellings, H. Kazemi-Kamyab, P. Nielsen, and L. Van den Abeele, "Classification and milling increase fly ash pozzolanic reactivity," *Frontiers in Built Environment*, vol. 7:670996, 2021. doi: https://doi.org/10.3389/fbuil.2021.670996

[70] K. Boakye and M. Khorami, "Impact of low-reactivity calcined clay on the performance of fly ash-based geopolymer mortar," *Sustainability*, vol. 15, no. 18, 2023. doi: https://doi.org/10.3390/su151813556

[71] A. Poowancum and P. Aengchuan, "Utilisation of low-reactivity fly ash for fabricating geopolymer materials," *Advances in Cement Research*, vol. 35, no. 4, pp. 144–151, 03 2022. doi: https://doi.org/10.1680/jadcr.21.00025

[72] F. Škvára, T. Jílek, and L. Kopecký, "Geopolymer materials based on fly ash," *Ceramics-Silikáty*, vol. 49, no. 3, pp. 195–204, 2005.

[73] X.-s. Lv, Y. Qin, Z.-x. Lin, Z.-k. Tian, and X.-m. Cui, "Inhibition of efflorescence in na-based geopolymer inorganic coating," *ACS Omega*, vol. 5, no. 24, pp. 14 822–14 830, 2020. doi: https://doi.org/10.1021/acsomega.0c01919

[74] C. N. Djangang, J. A. Mbey, C. J. Ekani, S. T. Tiam, P. Blanchart, and D. Njopwouo, "Improved microstructure and free efflorescence geopolymer binders," *SN Applied Sciences*, vol. 2, no. 12, p. 2167, Dec 2020. doi: https://doi.org/10.1007/s42452-020-03959-6

[75] L. Simão, E. Fernandes, D. Hotza, M. Ribeiro, O. Montedo, and F. Raupp-Pereira, "Controlling efflorescence in geopolymers: A new approach," *Case Studies in Construction Materials*, vol. 15, p. e00740, 2021. doi: https://doi.org/10.1016/j.cscm.2021.e00740

[76] Y. Ge, X. Tian, D. Huang, Q. Zhong, Y. Yang, and H. Peng, "Understanding efflorescence behavior and compressive strength evolution of metakaolin-based geopolymer under a pore structure perspective," *Journal of Building Engineering*, vol. 66, p. 105828, 2023. doi: https://doi.org/10.1016/j.jobe.2023.105828

[77] Y. Huang, "Influence of calcium bentonite addition on the compressive strength, efflorescence extent and drying shrinkage of fly-ash based geopolymer mortar," *Transactions of the Indian Ceramic Society*, vol. 79, no. 2, pp. 77–82, 2020. doi: https://doi.org/10.1080/0371750X.2020.1719206

[78] K. Kim, H. Song, S. Lee, H. Cho, H. M. Lim, and H. Ko, "Accentuating the ambient curing behavior of geopolymers: metamodel-guided optimization for fast-curing geopolymers with high flexural strength," *Digital Discovery*, vol. 4, pp. 653–665, 2025. doi: http://dx.doi.org/10.1039/D4DD00217B

[79] K. Arbi, M. Nedeljković, Y. Zuo, and G. Ye, "A review on the durability of alkali-activated fly ash/slag systems: Advances, issues, and perspectives," *Industrial & Engineering Chemistry Research*, vol. 55, no. 19, pp. 5439–5453, 2016. doi: https://doi.org/10.1021/acs.iecr.6b00559

[80] P. Mokhtari, A. Ozer, R. A. de Sá Ribeiro, D. Samuel, and W. M. Kriven, "Investigation of geopolymer efflorescence durability problems: Causes and possible solutions," *Journal of the American Ceramic Society*, vol. 107, no. 8, pp. 5364–5382, 2024. doi: https://doi.org/10.1111/jace.19830

[81] X. Hui, C. Li, J. Yan, H. Yu, H. Kan, Y. Tang, Q. Meng, and P. Dong, "Efflorescence suppression and performance enhancement in CaO-activated lepidolite lithium slag-based geopolymers," *Industrial & Engineering Chemistry Research*, vol. 65, no. 3, pp. 1621–1634, Jan 2026. doi: https://doi.org/10.1021/acs.iecr.5c03920

[82] A. Naghizadeh, L. Tchadjie, F. Solomon, S. Ekolu, C. Wu, and M. Welman-Purchase, "Efflorescence and strength effects of different ambient regimes of curing fly ash – based geopolymer concrete," *Construction and Building Materials*, vol. 516, p. 145722, 2026. doi: https://doi.org/10.1016/j.conbuildmat.2026.145722

[83] Z. Zhang, J. L. Provis, A. Reid, and H. Wang, "Fly ash-based geopolymers: The relationship between composition, pore structure and efflorescence," *Cement and Concrete Research*, vol. 64, pp. 30–41, 2014. doi: https://doi.org/10.1016/j.cemconres.2014.06.004

[84] J. Tan, Özlem Cizer, B. Vandevyvere, J. De Vlieger, H. Dan, and J. Li, "Efflorescence mitigation in construction and demolition waste (CDW) based geopolymer," *Journal of Building Engineering*, vol. 58, p. 105001, 2022. doi: https://doi.org/10.1016/j.jobe.2022.105001

[85] K. Pasupathy, S. Ramakrishnan, and J. Sanjayan, "Effect of hydrophobic surface-modified fine aggregates on efflorescence control in geopolymer," *Cement and Concrete Composites*, vol. 126, p. 104337, 2022. doi: https://doi.org/10.1016/j.cemconcomp.2021.104337

[86] M. G. Plaza, S. Martínez, and F. Rubiera, "$CO_2$ capture, use, and storage in the cement industry: State of the art and expectations," *Energies*, vol. 13, no. 21, 2020. doi: https://doi.org/10.3390/en13215692

[87] P. van Tonder and M. S. Low, "The effect of $CO_2$ loading on the properties of normal concrete vs fly ash concrete," *Journal of Engineering, Design and Technology*, vol. 19, no. 6, pp. 1472–1487, 05 2021. doi: https://doi.org/10.1108/JEDT-08-2020-0315

[88] Z. Liu, "Effect of carbon dioxide curing on the carbonation durability of concrete," *Frontiers in Sustainable Development*, vol. 4, no. 8, pp. 46–52, Aug. 2024. doi: https://doi.org/10.54691/32xrdt215

[89] G. Centi, S. Perathoner, and G. Papanikolaou, "Plasma assisted $CO_2$ splitting to carbon and oxygen: A concept review analysis," *Journal of $CO_2$ Utilization*, vol. 54, p. 101775, 2021. doi: https://doi.org/10.1016/j.jcou.2021.101775

[90] D. S. Vijayan, S. Gopalaswamy, A. Sivasuriyan, E. Koda, W. Sitek, M. D. Vaverková, and A. Podlasek, "Advances and applications of carbon capture, utilization, and storage in civil engineering: A comprehensive review," *Energies*, vol. 17, no. 23, 2024. doi: https://doi.org/10.3390/en17236046

[91] S. A. Miller, A. Horvath, and P. J. M. Monteiro, "Readily implementable techniques can cut annual $CO_2$ emissions from the production of concrete by over 20%," *Environmental Research Letters*, vol. 11, no. 7, p. 074029, jul 2016. doi: https://doi.org/10.1088/1748-9326/11/7/074029

[92] C. Pade and M. Guimaraes, "The $CO_2$ uptake of concrete in a 100 year perspective," *Cement and Concrete Research*, vol. 37, no. 9, pp. 1348–1356, 2007. doi: https://doi.org/10.1016/j.cemconres.2007.06.009

[93] W.-Y. Wu, M. Zhang, C. Wang, L. Tao, J. Bu, and Q. Zhu, "Harnessing ash for sustainable $CO_2$ absorption: Current strategies and future prospects," *Chemistry – An Asian Journal*, vol. 19, no. 12, p. e202400180, 2024. doi: https://doi.org/10.1002/asia.202400180

[94] B. Jouamai, H. Elminor, and A. Belabid, "Challenges of carbon sequestration in construction materials — a scoping review," *Journal of Building Engineering*, vol. 114, p. 114349, 2025. doi: https://doi.org/10.1016/j.jobe.2025.114349

[95] E. A. E. Hamed, S. A. Khan, A. Yousaf, and M. Koç, "A comprehensive review of carbon capture, storage, and reduction strategies within the built environment," *Materials*, vol. 18, no. 24, 2025. doi: https://doi.org/10.3390/ma18245646

[96] S. Gupta and H. W. Kua, "Factors determining the potential of biochar as a carbon capturing and sequestering construction material: Critical review," *Journal of Materials in Civil Engineering*, vol. 29, no. 9, p. 04017086, 2017. doi: https://doi.org/10.1061/(ASCE)MT.1943-5533.0001924

[97] J.-L. Gálvez-Martos, R. Chaliulina, E. Medina-Martos, A. Elhoweris, A. Hakki, J. Mwanda, and Y. Al-Horr, "Eco-efficiency of a novel construction material produced by carbon capture and utilization," *Journal of $CO_2$ Utilization*, vol. 49, p. 101545, 2021. doi: https://doi.org/10.1016/j.jcou.2021.101545

[98] S. Brunauer, P. H. Emmett, and E. Teller, "Adsorption of gases in multimolecular layers," *Journal of the American Chemical Society*, vol. 60, no. 2, pp. 309–319, 1938. doi: https://doi.org/10.1021/ja01269a023